PHYSICAL REVIEW B **88**, 140402(R) (2013)

Memory effects on the magnetic behavior of assemblies of nanoparticles with ferromagnetic core/antiferromagnetic shell morphology

M. Vasilakaki,[1] K. N. Trohidou,[1] D. Peddis,[2] D. Fiorani,[2] R. Mathieu,[3] M. Hudl,[3] P. Nordblad,[3] C. Binns,[4] and S. Baker[4]

[1]*IAMPPNM, Department of Materials Science, NCSR "Demokritos," Aghia Paraskevi, 15310 Athens, Greece*

[2]*ISM–CNR, Area della Ricerca, Via Salaria km 29 500, C.P. 10-00016 Monterotondo Scalo, Roma, Italy*

[3]*Department of Engineering Sciences, Uppsala University-Box 534, SE-751 21 Uppsala, Sweden*

[4]*Department of Physics and Astronomy, University of Leicester, Leicester LE1 7RH, United Kingdom*

(Received 4 June 2013; revised manuscript received 23 July 2013; published 9 October 2013)

Monte Carlo simulations of the dynamic magnetic behavior of an assembly of ferromagnetic core/antiferromagnetic shell nanoparticles are reported and compared with the experimental results on a system of Co nanoparticles in Mn matrix. Memory effects on low-field zero-field-cooled magnetization curves have been investigated. Our simulations show that the memory effects increase with the concentration and that both the interface exchange coupling and the dipolar interparticle interactions contribute to the observed dynamic behavior. In particular the interface exchange interaction provides an additive source for the frustration of the system resulting in an enhancement of the memory effect. The numerical data reproduce well the experimental results confirming the glassy behavior of the investigated nanoparticle systems.

DOI: 10.1103/PhysRevB.88.140402 PACS number(s): 75.75.−c, 75.40.Mg, 75.30.Gw, 75.50.Tt

I. INTRODUCTION

Many dense magnetic nanoparticle systems exhibit slow dynamics which is qualitatively indistinguishable from that observed in atomic spin glasses, and its origin is attributed to strong dipolar interactions among particle moments.[1,2] The presence of dipolar interaction in such randomly distributed nanoparticle assemblies of high enough packing density combined with random orientation of anisotropy axes creates a competition of different spin alignments leading to a collective freezing of particle moments in a disordered magnetic state known as superspin glass (SSG).[1–4] The field-cooled (FC) and zero-field-cooled (ZFC) magnetization curves of SSG systems indicate the existence of nonequilibrium spin-glass characteristics such as aging, memory, and rejuvenation.[5]

However, slow dynamics has been also observed below a characteristic temperature (blocking temperature T_b) in dilute nanoparticle systems with weakly interacting superspins. In these systems the magnetic dipolar interaction energy between the nanoparticles is small compared to the anisotropy energy of the individual nanoparticles in the assembly. These systems basically behave above T_b as the superparamagnetic ones and the dynamic behavior follows the Néel-Brown[6] model. The field-cooled susceptibility continues to increase with decreasing temperature showing a superparamagnetic-like behavior.[1,7] In the literature aging and memory effects have been observed in the FC magnetization curves[8] of noninteracting assemblies and they are attributed to the size or anisotropy energy barriers' distribution, to the magnetic order of nanoparticles,[7] or the temperature driven dynamics[1,9,10] of the assembly. On the other hand, in SSG systems the FC magnetization curve below T_f, defined as the maximum of ZFC, either becomes temperature independent or shows a small maximum and then remains constant upon further cooling[4] while both FC and ZFC magnetization curves show slow dynamics. In the last few years, numerical and experimental results[8,11,12] have shown aging and memory effects in both FC and ZFC magnetization curves in systems of diluted nanoparticles. Such effects have been attributed to the surface spin-glass-like state resulting in each nanoparticle from spin frustration and high random anisotropy at the surface.[13]

In this context, the dynamic properties of size-selected gas-phase nanoparticles in the size range 1–10 nm embedded in a host magnetic matrix (nanocomposite) have recently become an object of great interest from both fundamental[14] and technological points of view.[15]

In this Rapid Communication we report our Monte Carlo (MC) simulations results in assemblies of nanoparticles with ferromagnetic (FM) core/antiferromagnetic (AFM) shell morphology for 5% and 10% particle concentrations. Our study is focused on ZFC-memory effects caused by aging the system at a certain temperature. The factors that influence the memory effects in the system are systematically studied. Our simulations show that the combined effect of intraparticle and interparticle interactions results in a high degree of frustration in the system and that generates spin-glass-like memory features. The memory effect is larger when the aging lasts longer and increases with increasing particles' concentration. The simulation results are compared with experimental findings on the Co nanoparticles embedded in an antiferromagnetic Mn matrix where a strong interface exchange coupling between Co and Mn exists.[16–18]

II. THE MODEL

We consider an assembly of N spherical nanoparticles, each of them having FM core/AFM shell morphology, located randomly on the nodes of a hexagonal lattice inside a box. The particle assembly is assumed monodispersed in accordance with the low size dispersion characterizing films grown by cluster beam technique.[17]

We consider spherical nanoparticles with diameter a. The nanoparticle i in the assembly consists of four regions: a FM core which is given by a macrospin $\vec{s}_{1i}$ with uniaxial anisotropy along the z axis, a FM interface given by a macrospin $\vec{s}_{2i}$, and an AFM interface given by two macrospins $\vec{s}_{3i}$, $\vec{s}_{4i}$, both having uniaxial anisotropy along the z axis and an AFM

shell corresponding to the macrospins $\vec{s}_{5i}$, $\vec{s}_{6i}$ with randomly oriented anisotropy axes. The spins inside each nanoparticle are exchange coupled. The particles in the assembly interact via dipolar forces. Dipolar interactions are the dominant interparticle interactions for the concentrations of 5% and 10% that are below the percolation threshold and then the direct exchange coupling between the nanoparticles is ignored.

Under these assumptions the total energy of the nanoparticles assembly is given as[17,19]

$$
\begin{aligned}
E = & -J_c \sum_{i=1}^{N} \vec{s}_{1i}\vec{s}_{2i} - J_{\mathrm{IF}} \sum_{i=1}^{N} (\vec{s}_{2i}\vec{s}_{3i} + \vec{s}_{2i}\vec{s}_{4i}) \\
& - J_{\mathrm{SH}} \sum_{i=1}^{N} (\vec{s}_{3i}\vec{s}_{4i} + \vec{s}_{3i}\vec{s}_{5i} + \vec{s}_{4i}\vec{s}_{6i} + \vec{s}_{5i}\vec{s}_{6i}) \\
& - K_c \sum_{i=1}^{N} (\vec{s}_{1i}\hat{e}_{1i})^2 \\
& - K_{\mathrm{IF}} \sum_{i=1}^{N} [(\vec{s}_{2i}\hat{e}_{2i})^2 + (\vec{s}_{3i}\hat{e}_{3i})^2 + (\vec{s}_{4i}\hat{e}_{4i})]^2 \\
& - K_{\mathrm{SH}} \sum_{i=1}^{N} [(\vec{s}_{5i}\hat{e}_{5i})^2 + (\vec{s}_{6i}\hat{e}_{6i})^2] - \sum_{i=1}^{N}\sum_{n=1}^{6} (\vec{s}_{ni}\vec{H}) \\
& + \frac{1}{2} \sum_{\substack{i,j=1 \\ j\neq i}}^{N} \sum_{n,k=1}^{6} \left[\frac{\vec{s}_{ni}\vec{s}_{kj}}{R_{ij}^3} - \frac{3(\vec{s}_{ni}\vec{R}_{ij})(\vec{s}_{ki}\vec{R}_{ij})}{R_{ij}^5} \right], \qquad (1)
\end{aligned}
$$

where $\vec{s}_{ni}$,$\vec{s}_{kj}$ (with the indices n and $k = 1,2,\ldots,6$) are the macrospins of the ith and jth particle, respectively, and $\hat{e}_{ni}$ is the corresponding anisotropy easy axis direction.

The first three terms correspond to the intraparticle interactions of the spins inside the nanoparticle, namely the nearest neighbor Heisenberg exchange interaction in the core, at the interface, and in the shell. The next three terms correspond to the anisotropy energy of the core, the interface, and the shell. The two last terms are the Zeeman energy and the dipolar energy of the system.

The energy parameters entering Eq. (1) are the intraparticle exchange energy strengths J_C of the core, J_{IF} of the interface, and J_{SH} of the shell, the anisotropy energy strengths K_C of the core, K_{IF} of the interface, and K_{SH} of the shell. These parameters for the anisotropy and exchange interaction strength are based on the bulk values of Co and Mn (Ref. 17) but they are modified from these bulk values because of the reduced size of the nanoparticles and the reduced symmetry along the interface and the surface.[20] Also the degree of alloying along the Co/Mn interface which has been determined by the extended x-ray absorption fine structure (EXAFS) measurements[17] on Co nanoparticles in a Mn matrix has been taken into account. In the simulations the anisotropy strengths of the interface and the shell are scaled with the core anisotropy strength $K_C = 0.1$, so $K_{\mathrm{IF}} = 0.5$ is taken five times bigger than K_C and $K_{\mathrm{SH}} = 1.0$, one order of magnitude bigger than K_C. $J_C = 1.0$ is taken as the reference value of the pure FM core and the other exchange strengths for the FM/AFM interface and the AFM shell as $J_{\mathrm{IF}} = 0.5$, $J_{\mathrm{SH}} = -0.5$.

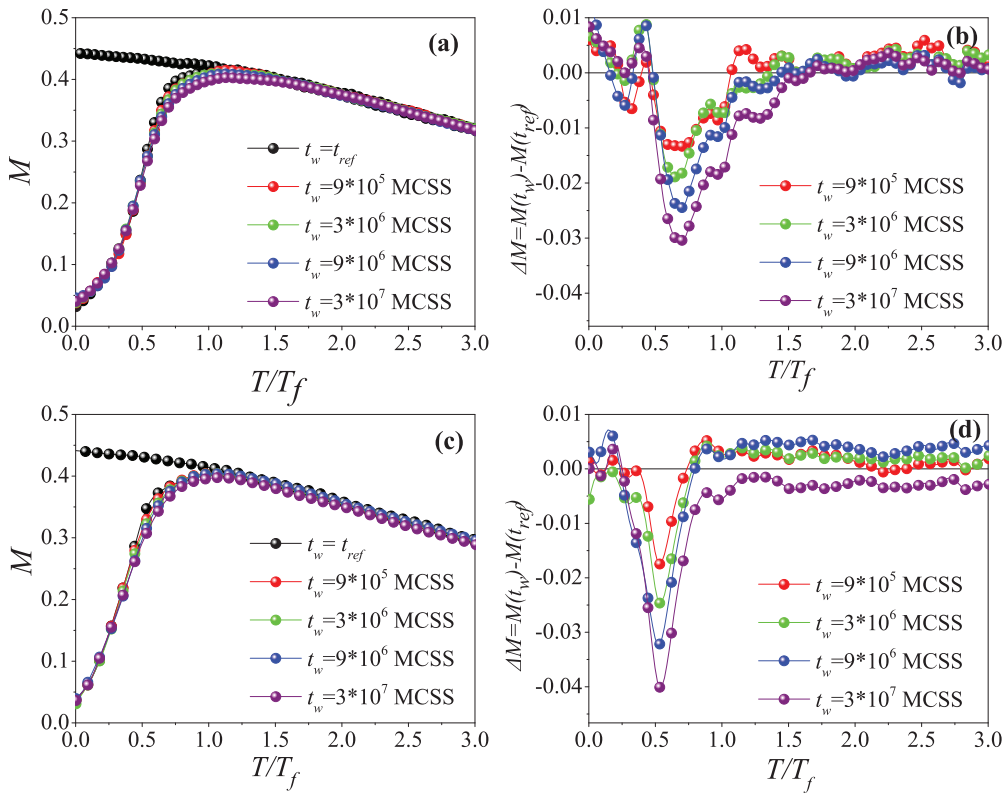

FIG. 1. (Color) ZFC-FC reference curve ($t_{\mathrm{ref}} = 3 \times 10^3$ MCSS) and ZFC-memory curves after stop-and-wait for t_w at $T/T_f = 0.64$ for 5% (a) and at $T/T_f = 0.5$ for 10% (c) concentration of the FM/AFM nanoparticle assemblies and $H = 0.20\ J_C/g\mu_B$. Difference between ZFC-reference and ZFC-memory curve as a function of temperature for different waiting times t_w for 5% (b) and 10% (d) concentration.

The applied magnetic field H is expressed in dimensionless units of $J_C/g\mu_B$ and the temperature T in units J_C/k_B. The field H is applied along the easy axis direction (z axis) of the anisotropy of the core and the interface where the magnetization M normalized to M_s is calculated.

For the calculation of the temperature-dependent magnetization curves, we have used the Monte Carlo simulation technique with the implementation of the METROPOLIS algorithm. The dipolar sums are calculated by the Ewald method.[21] At this point we have to note that the time evolution of the system does not come from any deterministic equation for the magnetization, the dynamics obtained is intrinsic to the MC method. This means that our time unit is not related to a real time interval. We focus on the effect of the concentration and the core/shell morphology on the dynamics and the qualitative agreement with the experimental results.

In the Monte Carlo method, during each Monte Carlo step, which is our time unit, we select a nanoparticle from the N nanoparticles of the assembly at random. Inside the selected nanoparticle we make a small change in the spins' orientation. The attempted change is accepted with a certain probability that corresponds to the Boltzmann probability and the magnetization of the system is updated.[22] In our simulations, for every temperature and applied field value, the system is allowed to relax from an initial spin configuration towards equilibrium for a reference time $t_{\rm ref} = 3 \times 10^3$ Monte Carlo steps per spin (MCSS). The first 1000 MCSS are used for equilibration of the system and the subsequent 2000 MCSS are used to calculate the thermodynamic average of the magnetization. The results are averaged over 30 samples with different spin configurations, random shell anisotropy axes, and spatial configurations for the nanoparticles.

For the calculation of the memory ZFC magnetization curves we use a procedure similar to the experimental one given in Refs. 1 and 23: We start cooling the system at a constant step rate from temperature $T = 150\ J_C/k_B$ down to the stop temperature (T_s) which is well below the freezing temperature, without the application of a field. At the temperature T_s, the system is aged for a waiting time t_w that ranges from 9×10^5 to 3×10^7 MCSS, a few orders of magnitude larger than the reference time, $t_{\rm ref}$. The cooling is then resumed down to the lowest temperature where a small magnetic field is applied ($H = 0.20\ J_C/g\mu_B$), and the memory ZFC magnetization is calculated during the heating process. A reference ZFC curve is also obtained for $t_w = t_{\rm ref}$ during the cooling process.

III. RESULTS AND DISCUSSION

We have calculated by MC simulations the memory effect for two particle concentrations of the FM/AFM nanoparticle assemblies. The calculated ZFC-FC reference magnetization curves and the ZFC-memory curves for different waiting times t_w are shown in Figs. 1(a) and 1(c), for 5% and 10% concentration, respectively, on a normalized temperature scale. The reference ZFC curves exhibit broad maxima at $T_f \sim 14\ J_C/k_B$ (5% sample) [Fig. 1(a)] and $T_f \sim 17\ J_C/k_B$ (10% sample) [Fig. 1(c)] that are defined as the freezing temperatures. We have calculated the memory ZFC magnetization curves after stop-and-wait in zero field at $T_s = 9\ J_C/k_B$ for waiting times $t_w = 9 \times 10^5$, 3×10^6, 9×10^6, and 3×10^7 MCSS (300, 1000, 3000, and 10 000 times larger than the reference time $t_{\rm ref}$, respectively) after the application of a low field $H = 0.20\ J_C/g\mu_B$. A memory dip is observed around the stop temperature for 5% at $T/T_f = 0.64$ and 10% concentration for $T/T_f = 0.5$. Because this dip is small, we examine also the behavior of the difference $\Delta M = M(t_w) - M(t_{\rm ref})$ between the aged and the normal ZFC magnetization as a function of temperature for both concentrations [Figs. 1(b) and 1(d)].

In Figs. 1(a) and 1(c) we observe that FC reference curves increase weakly as temperature decreases and become flat at very low temperature, indicating a spin-glass-like behavior.[5] ZFC-memory curves lie below the reference curve at temperatures close to the stop temperature T_s. We observe that memory dips exist around T_s where the system was allowed to relax during the cooling procedure. The memory effect depends on the t_w and on the nanoparticles' concentration and this becomes clear from the minimum in the difference plot ΔM at about T_s. This difference indicates that the magnetic moment configuration spontaneously rearranges towards lower energy configurations when the system is left unperturbed at constant temperature T_s during the cooling process. The lower energy configuration becomes frozen on further cooling and is retrieved on reheating. The system goes into deeper and deeper valleys with increasing energy barriers as the waiting time increases.[24] The fact that reference and stop-and-wait curves

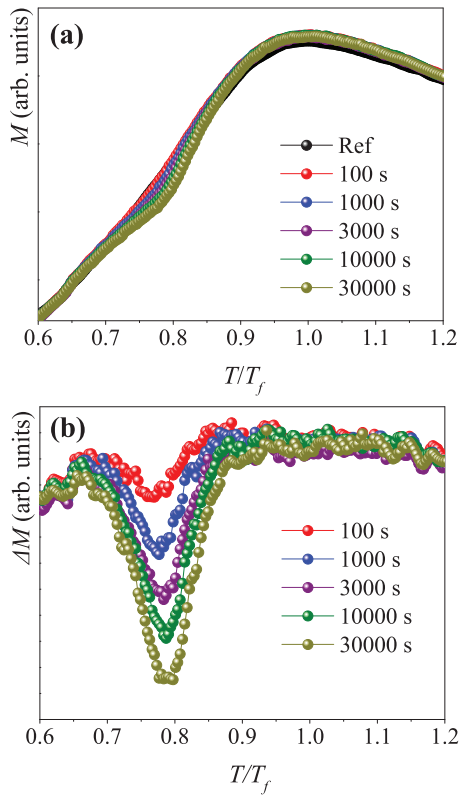

FIG. 2. (Color) (a) Experimental data of the ZFC-reference curve (open circles) and ZFC-memory curves for a stop-and-wait between 100 and 30 000 s at $T = 55$ K ($\sim 0.8T_f$) for 9.8% concentration of a system of Co nanoparticles in a Mn matrix (Ref. 26). (b) Difference between ZFC-reference and ZFC-memory curve with waiting times between 100 and 30 000 s.

coalesce at low temperatures and only start to deviate as T_s is approached from below clearly indicates that the rejuvenation of the system occurs as the temperature is decreased away from T_s in the stop-and-wait protocol as is the case for superspin glasses.[3] We also observe that decreasing the concentration, and thus the dipolar interaction strength, the memory dips become smaller and broader indicating the role of the dipolar interactions on memory effect.

The simulation data are compared with the experimental results on a Co in Mn matrix system[17] where particles consist of a Co-rich ferromagnetic core in contact with a Co-depleted antiferromagnetic shell fading into the AFM Mn matrix. The Co particles in Mn matrix samples were prepared in thin film form by codeposition using a gas aggregation cluster source[25] and a molecular beam epitaxy (MBE) source. The cluster source produces a narrow size distribution of particle sizes (with $\langle D \rangle \cong 1.8$ nm, as measured *in situ* by an axially mounted quadrupolar filter). ZFC and FC magnetization measurements were performed using a superconducting quantum interference device (SQUID) magnetometer (Quantum Design MPMS). In all experiments the temperature $T = 150$ K was used as the reference temperature. This temperature is well above the freezing temperature of $T_f = 70$ K where the samples exhibit pure superparamagnetic behavior.

Memory and rejuvenation effects of the ZFC magnetization after a stop-and-wait for 10^4 s at approximately $0.8T_f$ are observed at 4.7% and 9.8% concentration in Ref. 26, close to the case for our simulated system. The experimental ZFC-reference magnetization curves and the ZFC-memory curves for different waiting times t_w are shown in Fig. 2(a) for a concentration of 9.8%. The $\Delta M(T)$ curve [Fig. 2(b)] shows the logarithmic character of the slow dynamics in agreement with our numerical results for the particle concentration of 10%. In addition, for a logarithmic spacing of waiting times in our simulations, we obtain equally spaced depths in the calculated memory dips [Fig. 1(d)] in agreement with the experimental data [Fig. 2(b)].[26]

In order to further investigate the contribution of the dipolar interaction and the exchange interface interaction to the memory effect, we switch off the dipolar interactions in the MC simulations in the case of the 10% concentration calculating the ZFC and the memory ZFC curves for the various waiting times [Fig. 3(a)] together with the ΔM curve as a function of temperature [Fig. 3(b)]. We keep the same stop temperature T_s and cooling field value as in the calculations appearing in Figs. 1(c) and 1(d). We must notice here that in our simulation we find that in the absence of dipolar interactions the freezing temperature T_f is decreasing[19] consequently the ratio T/T_f increases.

In Fig. 3(b) we observe that a memory effect still exists, although much weaker from the memory effect observed in the system with the interparticle dipolar interactions [see Fig. 1(d)], indicating that the interface exchange interaction contributes to this effect. The frustration that exists at the

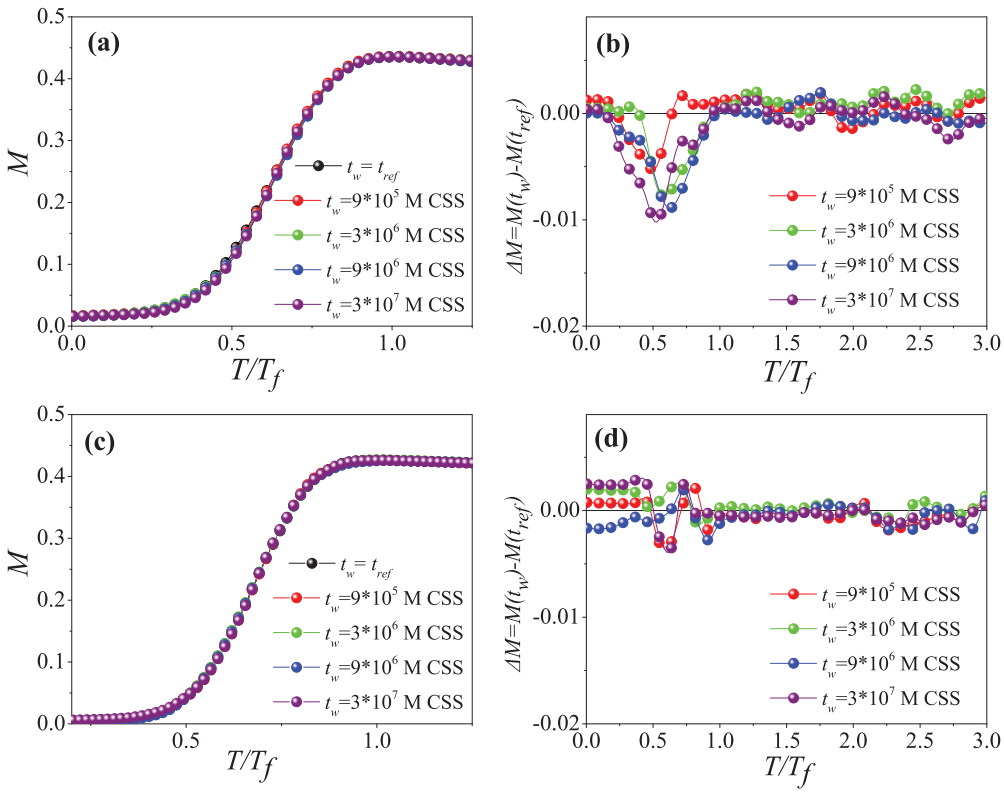

FIG. 3. (Color) (a) ZFC-reference curve ($t_{\rm ref} = 3 \times 10^3$ MCSS) and ZFC-memory curves after stop-and-wait for t_w at $T/T_f = 0.72$ for FM/AFM nanoparticles' concentration 10% and $H = 0.20\ J_C/g\mu_B$ without the presence of dipolar interactions. (b) Difference between ZFC-reference and ZFC-memory curve for different waiting times t_w. (c) ZFC-reference and ZFC-memory curves after stop-and-wait for t_w at $T/T_f = 0.82$ for FM/AFM nanoparticles' concentration 10% and $H = 0.20\ J_C/g\mu_B$ without the presence of dipolar interactions and exchange interface coupling. (d) Difference between ZFC-reference and ZFC-memory curve for different waiting times t_w in this case.

interface between the ferromagnetic spin at the core interface and the antiferromagnetic spins at the shell interface creates this small memory effect. This is further confirmed from Figs. 3(c) and 3(d) where we have plotted the memory ZFC curves and the $\Delta M(T)$ curve, respectively, for various waiting times t_w switching off both the interparticle and the intraparticle interactions. We see that the memory effect in this case is negligible indicating that the synergy between these two types of interactions is responsible for it.

IV. CONCLUSIONS

We have performed Monte Carlo simulations to study the memory effect on ZFC magnetization curves in an assembly of FM core/AFM shell nanoparticle assemblies including both interparticle dipolar interactions and intraparticle exchange coupling. The results are compared with the experimental findings on Co nanoparticles embedded in a Mn matrix. These Co/Mn nanocomposites of 4.7% and 9.8% concentration show spin-glass-like behavior and the MC simulations well reproduce the experimentally observed memory effect during aging of the systems at a certain temperature in zero-field cooling. A memory dip of finite width around the stop temperature is observed in the simulations on reheating, confirming the spin-glass-like behavior. Outside this temperature range, the magnetization recovers its reference level and the system appears to be rejuvenated. The depth of the memory dip increases with increasing waiting time and it becomes more pronounced with increasing nanoparticles' concentration. The MC simulations show that dipolar interparticle interactions combined with interface exchange interactions create a highly frustrated system that generates spin-glass-like memory features.

ACKNOWLEDGMENTS

This research has been cofinanced by the European Social Fund (EU) and Greek national funds through the Operational Program "Education and Lifelong Learning" in the framework of ARISTEIA I (Project No. COMANA/22).

[1] M. Sasaki, P. E. Jönsson, H. Takayama, and H. Mamiya, Phys. Rev. B **71**, 104405 (2005).
[2] M. Ulrich, J. García-Otero, J. Rivas, and A. Bunde, Phys. Rev. B **67**, 024416 (2003).
[3] S. Sahoo, O. Petracic, W. Kleemann, P. Nordblad, S. Cardoso, and P. P. Freitas, Phys. Rev. B **67**, 214422 (2003).
[4] O. Petracic, X. Chen, S. Bedanta, W. Kleemann, S. Sahoo, S. Cardoso, and P. P. Freitas, J. Magn. Magn. Mater. **300**, 192 (2006).
[5] D. Parker, V. Dupuis, F. Ladieu, J.-P. Bouchaud, E. Dubois, R. Perzynski, and E. Vincent, Phys. Rev. B **77**, 104428 (2008).
[6] L. Néel, Ann. Geophys. (C.N.R.S.) **5**, 99 (1949); W. F. Brown, Jr., Phys. Rev. **130**, 1677 (1963).
[7] S. K. Mishra, Eur. Phys. J. B **78**, 65 (2010).
[8] V. Bisht and K. P. Rajeev, J. Phys.: Condens. Matter **22**, 016003 (2010).
[9] G. M. Tsoi, L. E. Wenger, U. Senaratne, R. J. Tackett, E. C. Buc, R. Naik, P. P. Vaishnava, and V. Naik, Phys. Rev. B **72**, 014445 (2005).
[10] D. De, A. Karmakar, M. K. Bhunia, A. Bhaumik, S. Majumdar, and S. Giri, J. Appl. Phys. **111**, 033919 (2012).
[11] K. N. Trohidou, M. Vasilakaki, D. Peddis, and D. Fiorani, IEEE Trans. Magn. **48**, 1305 (2012).
[12] R. J. Tackett, A. W. Bhuiya, and C. E. Botez, Nanotechnology **20**, 445705 (2009).
[13] D. De, K. Dey, S. Majumdar, and S. Giri, Solid State Commun. **152**, 1857 (2012).
[14] V. Skumryev, S. Stoyanov, Y. Zhang, G. Hadjipanayis, D. Givord, and J. Nogues, Nature **423**, 850 (2003).
[15] S. Sun, Adv. Mater. **18**, 393 (2006); N. A. Frey, S. Peng, K. Cheng, and S. Sun, Chem. Soc. Rev. **38**, 2532 (2009).
[16] J. Nogués and I. K. Schuller, J. Magn. Magn. Mater. **192**, 203 (1999).
[17] C. Binns, N. Domingo, A. M. Testa, D. Fiorani, K. N. Trohidou, M. Vasilakaki, J. A. Blackman, A. M. Asaduzzaman, S. Baker, M. Roy, and D. Peddis, J. Phys.: Condens. Matter **22**, 436005 (2010).
[18] N. Domingo, D. Fiorani, A. M. Testa, C. Binns, S. Baker, and J. Tejada, J. Phys. D: Appl. Phys. **41**, 134009 (2008).
[19] G. Margaris, K. N. Trohidou, and J. Nogues, Adv. Mater. **24**, 4331 (2012).
[20] F. Bødker, S. Mørup, and S. Linderoth, Phys. Rev. Lett. **72**, 282 (1994).
[21] A. Grzybowski, E. Gwóźdź, and A. Bródka, Phys. Rev. B **61**, 6706 (2000).
[22] K. Binder and D. W. Heermann, *Monte Carlo Simulation in Statistical Physics, An Introduction*, Solid-State Sciences Vol. 80 (Springer-Verlag, Berlin, Heidelberg, 1988).
[23] R. Mathieu, M. Hudl, and P. Nordblad, Europhys. Lett. **90**, 67003 (2010).
[24] M. Bandyopadhyay and S. Dattagupta, Phys. Rev. B **74**, 214410 (2006).
[25] S. H. Baker, S. C. Thornton, K. W. Edmonds, M. J. Maher, C. Norris, and C. Binns, Rev. Sci. Instrum. **71**, 3178 (2000).
[26] D. Peddis, M. Hudl, C. Binns, D. Fiorani, and P. Nordblad, J. Phys.: Conf. Ser. **200**, 072074 (2010).